

PAPER

[View Article Online](#)
[View Journal](#) | [View Issue](#)Cite this: *Catal. Sci. Technol.*, 2021,
11, 1881**Tunable selectivity of phenol hydrogenation to cyclohexane or cyclohexanol by a solvent-driven effect over a bifunctional Pd/NaY catalyst†**Heng Xia,^a Hongzi Tan,^a ^{*a} Hongyou Cui,^a ^{*a} Feng Song,^a Yuan Zhang,^a
Rongrong Zhao,^a Zhe-Ning Chen,^a ^{*b} Weiming Yi^c and Zhihe Li^c

Hydrogenation of phenol is an important strategy to produce cyclohexane or cyclohexanol as both of them are raw materials for the synthesis of nylon-6 and nylon-66. Herein, we report a novel method for the selective hydrogenation of phenol to cyclohexane or cyclohexanol over a bifunctional Pd/NaY catalyst by regulating the solvent polarity. It was found that solvent polarity has a strong influence on the hydrogenation reaction mechanism. Under the identical conditions, 100% selectivity to cyclohexane could be obtained when reacting in *n*-octane (nonpolar solvent), while 92.3% selectivity to cyclohexanol was achieved in EtOH (polar solvent). The polarity of the solvent not only affects the competitive adsorption capacity but also the adsorption manner of phenol over the acid sites and the Pd nanoparticles in the Pd/NaY catalyst. DFT calculations show that different solvents have an almost negligible effect on the reaction energy barriers but highly affect the hydration reaction of cyclohexanol if the trace amount of water formed could not be timely removed from the catalytic system. This solvent-driven catalysis exhibits good recyclability, showing great promise for industrial applications. These findings not only provide new insights into the hydrogenation mechanism of phenolics, but also might help to develop facile strategies for the selective conversion of other phenolics into desired products.

Received 12th November 2020,
Accepted 20th December 2020

DOI: 10.1039/d0cy02188a

rsc.li/catalysis**1. Introduction**

Both cyclohexane and cyclohexanol are important chemical intermediates as they are widely used for the production of caprolactam for nylon-6 and adipic acid for nylon-66.^{1–3} On the industrial scale, cyclohexane is currently produced by hydrogenation of benzene, while cyclohexanol is derived from oxidation of cyclohexane.^{4–6} Although cyclohexane can be synthesized through hydrogenation of benzene, this process is less economical, and oxidation of cyclohexane to cyclohexanol is far from satisfactory because of the harsh reaction conditions.^{7,8} An attractive production route for cyclohexane and cyclohexanol is selective hydrogenation or hydrodeoxygenation of phenol through a one-step process, because such a catalytic system offers atom efficiency and energy sav-

ings.^{9,10} Besides, phenol can be obtained from biomass and coal refineries inexpensively.¹¹

Recently, it was reported that hydrogenation of phenol could be efficiently catalyzed by Pd-based catalysts, including Pd/C, Pd/MgO, Pd/SiO₂, Pd/Al₂O₃ and Pd/MOFs.^{12–17} The surface acid properties of supports also have an important influence on the catalytic performance.^{18,19} As reported by J. W. Zhong *et al.*, the acid sites on catalysts have the ability to enhance the chemisorption of phenol and promote the conversion rate.²⁰ P. Yan *et al.* found that the hydrogenation and dehydration reactions of guaiacol could be effectively catalyzed by metal sites and acid sites in Ni/Beta catalysts, respectively, affording cyclohexane as the major product.²¹ There was a linear relationship observed between deoxygenation activity and concentration of acid sites.²¹ Moreover, a combination of metals (Pd, Pt, and Ni) and liquid (H₃PO₄) or solid acid catalysts (Nafion, SO₄^{2–}/ZrO₂, HZSM-5 and HBEA) demonstrated high selectivity to cycloalkanes in the conversion of phenolic compounds.^{18,22–26} Over Pd-based catalysts supported on different oxides, whether hydrodeoxygenation or hydrogenation could take place highly depends on the presence or absence of acid sites.²⁷ Although a lot of effort has been devoted to developing high-performance catalysts, the catalytic mechanism of hydrodeoxygenation or hydrogenation of phenol still needs to be further clarified at the molecular level.

^a School of Chemistry & Chemical Engineering, Shandong University of Technology, Zibo, Shandong 255049, P. R. China. E-mail: hztan@sdu.edu.cn, cuihy@sdu.edu.cn^b State Key Laboratory of Structural Chemistry, Fujian Institute of Research on Structure of Matter, Chinese Academy of Sciences, Fuzhou, Fujian 350002, P. R. China. E-mail: znchen@fjirsm.ac.cn^c School of Agricultural Engineering and Food Science, Shandong University of Technology, Zibo, Shandong 255049, P. R. China

† Electronic supplementary information (ESI) available: Materials, catalyst preparation, catalyst characterization, catalyst evaluation, and computational methods and models. See DOI: 10.1039/d0cy02188a

Besides catalysts, the properties of used solvents are likely to affect the reaction pathway of phenol, as well as the reactivity.²⁸ It is well known that solvents have impact on the H₂ solubility in the liquid phase and thus on the reaction rate of phenol.²⁹ The competitive adsorption behavior of solvent and reactant molecules over the catalyst surface is probably altered by different solvents.³⁰ For example, selective hydrogenation of nitrobenzene to aniline or cyclohexylamine could be switched by using different solvents in the presence of a Pd/MIL-101 catalyst, because the solvent polarity is able to regulate the linkage between intermediates and the organic ligand in MIL-101.³¹ To better understand the catalytic mechanism of phenol conversion in different solvents, it is worthwhile to clarify the interactions of solvent molecules with the active sites on the catalyst, and the competitive adsorption behavior with the reactant, intermediates and products.

In this work, we reported a solvent-driven effect on the reaction pathway of phenol hydrogenation over a bifunctional Pd/NaY catalyst. The catalytic performance over different catalysts and in six solvents with different polarities was investigated. The catalysts were characterized by N₂ adsorption-desorption, inductively coupled plasma (ICP) spectroscopy, powder X-ray diffraction (PXRD), X-ray photoelectron spectroscopy (XPS), NH₃ temperature programmed desorption (NH₃-TPD), and X-ray absorption near-edge structure (XANES) and extended X-ray absorption fine structure (EXAFS) spectroscopy. Based on the kinetic experimental data, adsorption of phenol in different solvents and density functional theory (DFT) calculations, the effect of solvent polarity on the reaction pathway was analyzed and discussed.

2. Results and discussion

The textural structure information of the bifunctional Pd/NaY catalyst and its support NaY zeolite is summarized in Table 1. The Pd content in Pd/NaY measured by ICP was 1.98 wt%, which agrees very well with the designed value of 2.0 wt%. The N₂ adsorption-desorption isotherms at a temperature of 77 K were also obtained (Fig. S2†). Both the Pd/NaY catalyst and NaY zeolite exhibited similar type IV isotherms with BET areas of 576.83 m² g⁻¹ for Pd/NaY and 672.42 m² g⁻¹ for the NaY zeolite. As compared with the NaY zeolite (pore size: 3.93 nm, pore volume: 0.33 cm³ g⁻¹), the slight decrease in pore size (3.86 nm) and pore volume (0.28 cm³ g⁻¹) of the Pd/NaY catalyst exactly demonstrates that the deposited Pd species were uniformly loaded into the cavities of the NaY zeolite.

PXRD was employed to characterize the structure and crystallinity of the prepared Pd/NaY catalyst and the support

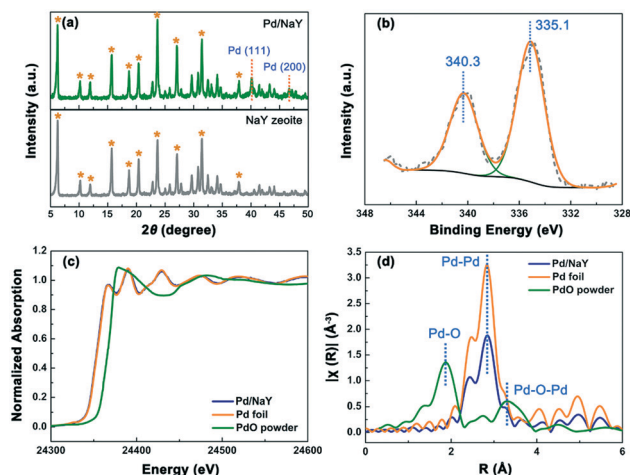


Fig. 1 (a) PXRD patterns of the Pd/NaY catalyst and NaY zeolite; (b) Pd 3d XPS spectra of the Pd/NaY catalyst; (c) normalized XANES spectra at the Pd K-edge of Pd foil, PdO powder, and the Pd/NaY catalyst; (d) Fourier transform spectra of the experimental EXAFS spectroscopy of Pd foil, PdO powder and the Pd/NaY catalyst.

(Fig. 1a). For the NaY zeolite, the diffraction signals at 6.3°, 10.1°, 11.9°, 15.8°, 18.7°, 20.5°, 23.7°, 27.2°, 31.4° and 37.9° were identified as the (111), (220), (311), (331), (511), (440), (533), (642), (555) and (666) lattice planes, respectively.^{32,33} The newly emerged diffraction signals at 40.2° and 46.7° of the Pd/NaY sample can be assigned to the {111} and {200} lattice planes of Pd nanoparticles,³⁴ indicating the successful deposition of Pd species on the NaY zeolite. XPS was performed to characterize the redox species of deposited Pd. As shown in Fig. 1b, the peaks at 340.3 eV and 335.1 eV are attributed to Pd 3d_{3/2} and Pd 3d_{5/2} of zerovalent Pd,³⁴ revealing that the deposited Pd species in Pd/NaY was in the metallic state. Moreover, the white line peak of the Pd/NaY catalyst in the XANES spectra (Fig. 1c) is nearly identical to that of Pd foil, and only the Pd-Pd bond signal appeared in the EXAFS spectrum of the Pd/NaY catalyst (Fig. 1d), both of which further unveil that the deposited Pd species in the Pd/NaY catalyst was in the form of nanoparticles, in accordance with the results of PXRD and XPS. In addition, the TEM and HRTEM images (Fig. 2) of the Pd/NaY catalyst exhibited that the Pd nanoparticles with the mainly exposed {111} crystal facets were uniformly dispersed on the support NaY zeolite.

To analyze the surface acid properties of Pd/NaY and Pd/SiO₂ as a counterpart, NH₃-TPD was conducted. As shown in Fig. 3, Pd/NaY presented a strong NH₃ desorption peak in the temperature range of 100–300 °C, while the Pd/SiO₂ catalyst did not show any NH₃ desorption in the whole tested temperature range. The strong NH₃ desorption peak of the Pd/NaY catalyst

Table 1 Textural structure information on the Pd/NaY catalyst and NaY zeolite

Samples	Designed Pd content (%)	Measured Pd content (%)	BET area (m ² g ⁻¹)	Pore size (nm)	Pore volume (cm ³ g ⁻¹)
Pd/NaY	2.0	1.98	576.83	3.86	0.28
NaY zeolite	—	—	672.42	3.93	0.33

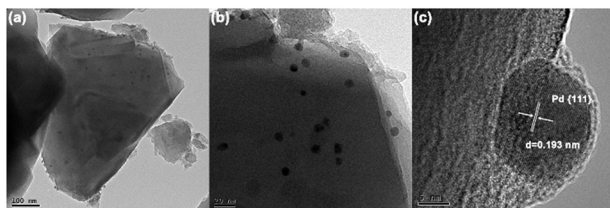


Fig. 2 TEM (a and b) and HRTEM (c) images of the Pd/NaY catalyst.

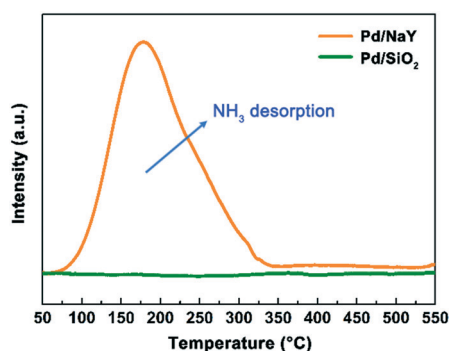


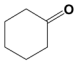
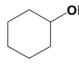
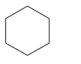
Fig. 3 NH_3 -TPD curves of the Pd/NaY catalyst and its counterpart Pd/ SiO_2 catalyst.

can be attributed to the surface acid sites in the NaY zeolite. It has been reported that the framework of the NaY zeolite is composed of AlO_4 (Al^{3+}) and SiO_4 (Si^{4+}) units, in which the framework charge is balanced by monovalent cations (such as Na^+ and H^+),³⁵ resulting in the large number of acid sites formed. The absence of acid sites in the Pd/ SiO_2 catalyst makes it an

ideal counterpart for comparing with Pd/NaY to judge the catalytic role of acid sites in the conversion of phenol.

The catalytic activity in the conversion of phenol was evaluated by using Pd/NaY, Pd/ SiO_2 and NaY zeolite as catalysts, respectively (Table 2). Six solvents with different polarities were examined including water (H_2O), *N,N*-dimethylformamide (DMF), methanol (MeOH), ethanol (EtOH), *n*-butanol (*n*-BuOH) and *n*-octane, whose polarities can be estimated by their dielectric constant order: H_2O (80.4) > DMF (38.3) > MeOH (33.6) > EtOH (24.3) > *n*-BuOH (17.8) > *n*-octane (2.1). Under the catalysis of the Pd/NaY catalyst, distinct differences in the phenol conversion and product selectivity were observed when using the solvents with different polarities. In strong polar solvents like H_2O (entry 1), DMF (entry 2) and MeOH (entry 3), no conversion of phenol was observed. It has been reported that the nonreactivity of phenol in MeOH is due to the MeOH adsorption on the Pd surface, as well as to the interaction between MeOH and the reactant molecules.³⁶ The polarity of H_2O is much stronger than that of MeOH, leading to a similar result. In addition to the strong polarity of DMF, the alkalescent amide groups in DMF might be also responsible for the nonreactivity of phenol, as it could further strengthen the interaction between the solvent and acid sites on the catalyst and the interaction between the solvent and phenol, leading to the absolute chemical inertness of phenol in DMF. In lower polarity EtOH (entry 4) compared to H_2O , MeOH and DMF, 78.2% phenol conversion was obtained, with 7.7% selectivity to cyclohexanone and 92.3% selectivity to cyclohexanol *via* the benzene-ring hydrogenation reaction. In the much less polar *n*-BuOH (entry 5), 62.4% selectivity to cyclohexanone and 37.6%

Table 2 Catalytic results of the conversion of phenol

						Selectivity (%)		
						Ring-hydrogenation		Hydrodeoxygenation
								
Entry	Catalyst	Reactant	Solvent	ϵ^a	Conversion (%)			
1 ^b	Pd/NaY	Phenol	H_2O	80.4	0	0	0	0
2 ^b	Pd/NaY	Phenol	DMF	38.3	0	0	0	0
3 ^b	Pd/NaY	Phenol	MeOH	33.6	0	0	0	0
4 ^b	Pd/NaY	Phenol	EtOH	24.3	78.2	7.7	92.3	0
5 ^b	Pd/NaY	Phenol	<i>n</i> -BuOH	17.8	68.7	62.4	37.6	0
6 ^b	Pd/NaY	Phenol	<i>n</i> -octane	2.1	100.0	0	0	100.0
7 ^b	NaY	Phenol	EtOH	24.3	0	0	0	0
8 ^b	NaY	Phenol	<i>n</i> -octane	2.1	0	0	0	0
9 ^b	Pd/ SiO_2	Phenol	EtOH	24.3	0	0	0	0
10 ^b	Pd/ SiO_2	Phenol	<i>n</i> -octane	2.1	54.2	69.3	25.4	5.2
11 ^b	Pd/NaY	Cyclohexanol	EtOH	24.3	12.0	0	—	100.0
12 ^b	Pd/NaY	Cyclohexanol	<i>n</i> -octane	2.1	100.0	0	—	100.0
13 ^c	Pd/NaY	Benzene	EtOH	24.3	15.2	0	0	100.0
14 ^c	Pd/NaY	Benzene	<i>n</i> -octane	2.1	100	0	0	100.0

^a Dielectric constant of the different solvents. ^b Reaction conditions: 0.1 g catalyst, 1.0 g reactants, 70 mL solvent, 5.0 MPa H_2 , 235 °C, 4.0 h.

^c Reaction conditions: 0.1 g catalyst, 1.0 g benzene, 70 mL solvent, 5.0 MPa H_2 , 235 °C, 2.0 h.

selectivity to cyclohexanol were obtained. When reacting in nonpolar *n*-octane (entry 6), phenol was completely transformed into cyclohexane with a selectivity of 100%, which indicates that the hydrodeoxygenation reaction occurred simultaneously. These results demonstrate that the reaction products can be regulated by the solvent effect.

In order to shed light on the catalytic role of metallic sites and acid sites on the bifunctional Pd/NaY catalyst, the catalytic activities of the NaY zeolite (with acid sites but no metallic sites) and Pd/SiO₂ (with metallic sites but no acid sites) were evaluated either in EtOH or in *n*-octane. Under the catalysis of the NaY zeolite, no phenol was transformed no matter which one of the reaction solvents was used (entry 7 & 8), proving that without metallic sites, the hydrogenation reaction could not take place as the hydrogenation of benzene-ring is a prerequisite for phenol conversion. Interestingly, in the solvent EtOH (entry 9), phenol could not be hydrogenated when using Pd/SiO₂ as the catalyst, despite demonstrating an excellent catalytic performance for many hydrogenation reactions.³⁷ When replacing EtOH with *n*-octane as the solvent (entry 10), however, 54.2% phenol conversion was achieved. These results clearly prove that the solvents play very important roles in the hydrogenation of phenol. In terms of product selectivity, in the reaction medium *n*-octane, Pd/SiO₂ afforded predominantly ring-hydrogenation products, cyclohexanone (69.3%) and cyclohexanol (25.4%), but the hydrodeoxygenation product (cyclohexane, 5.2%) was very low, indicating that the dehydration of cyclohexanol was prohibited due to the absence of acid sites.

To further verify the role of acid sites in the hydrodeoxygenation process, cyclohexanol was also used as the substrate and subjected to hydrogenation. In the EtOH solvent (entry 11), the conversion to cyclohexanol was only 12.0% in spite of the abundant acid sites on Pd/NaY, but it was enhanced to 100% in the *n*-octane solvent (entry 12). As we know, hydrogenation of cyclohexanol undergoes dehydration first and then hydrogenation, and cyclohexane is the unique product. Thus, the selectivity to cyclohexane should be 100% no matter what the conversion rate is. These results demonstrate that not only the acid sites but also the solvent polarity play a very crucial role in determining the reaction mechanism. Under the same reaction conditions, the hydrogenation of benzene in EtOH resulted in merely a cyclohexane yield of 15.2% (entry 13), but a cyclohexane yield of 100% was achieved in *n*-octane (entry 14). The much lower reactivities of cyclohexanol and benzene in EtOH as compared to those in *n*-octane reveal that the polarity of the solvent has a significant influence on the reaction rate. This can also be used to explain why no cyclohexane was formed in the hydrogenation of phenol when reacting in EtOH.

In an attempt to obtain more information on the reaction pathway, the kinetic study of phenol conversion over the Pd/NaY catalyst was carried out in *n*-octane and EtOH, respectively (Fig. 4). When reacting in nonpolar *n*-octane, as shown in Fig. 4a, cyclohexanone and cyclohexanol are the major intermediates as their concentrations presented a maximum with the reaction time. There are two pathways for phenol conversion as

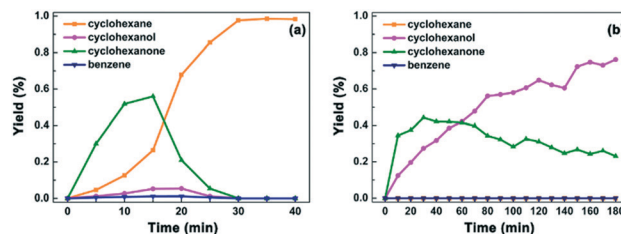
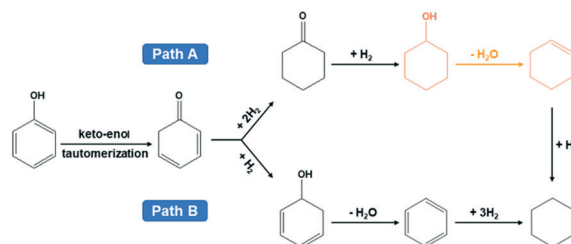


Fig. 4 The variation tendencies of product concentrations over the Pd/NaY catalyst in (a) *n*-octane and (b) EtOH as a function of time. Reaction conditions: 0.1 g catalyst, 1.0 g phenol, 70 mL solvent, 5.0 MPa H₂, 235 °C.

shown in Scheme 1. The high concentrations of cyclohexanone and cyclohexanol suggest that after the keto-tautomerization of phenol to cyclohexa-2,4-dien-1-one, consecutive hydrogenation of C=C bonds to cyclohexanone is the first step in path A, followed by hydrogenation of cyclohexanone to cyclohexanol and further hydrodeoxygenation to cyclohexane. The process of keto-tautomerization with cyclohexa-2,4-dien-1-one participating in phenol hydrogenation has been adequately demonstrated.²⁷ The concentration of cyclohexane increased slowly in the initial time, and increased rapidly with the consumption of cyclohexanol and benzene. A little amount of benzene could also be formed with a tendency to increase gradually at the early stage to a maximum and then declining due to the further hydrogenation to cyclohexane (Fig. S3a†). Such a time course tendency indicates that the reaction pathway of benzene hydrogenation to cyclohexane (path B) is also tenable but it is not the main reaction pathway. In path B, the C=O bond in cyclohexa-2,4-dien-1-one was first hydrogenated to produce cyclohexadienols, followed by dehydration of cyclohexadienols to benzene, and further benzene was hydrogenated to cyclohexane.

When reacting in polar EtOH (Fig. 4b and S3b†), however, the major products were cyclohexanone and cyclohexanol; almost no cyclohexane was formed. Such a case reveals that the hydrodeoxygenation of phenol is hard to take place in polar EtOH. The hydrogenation rate of phenol to cyclohexanone and cyclohexanol seemed lower than that when reacting in *n*-octane. Besides, no benzene was detected through the entire reaction course. These results provide evidence that hydrodeoxygenation reactions were prohibited by EtOH.

Combining with the poor conversion rate of benzene in the EtOH solvent (entry 13, Table 2), we conclude that path A is the only reaction pathway over the Pd/NaY catalyst in



Scheme 1 The proposed reaction pathway for phenol conversion.

EtOH, but the dehydration reaction of cyclohexanol is impeded.

In order to clarify which reaction pathway is mainly responsible for the formation of cyclohexane when reacting in nonpolar *n*-octane, cyclohexanol dehydration (path A) or benzene hydrogenation (path B), phenol conversion was examined under different H₂ pressures using *n*-octane as the solvent (Fig. 5). Under high H₂ pressure (5.0 MPa and 3.0 MPa), which allows sufficient hydrogenation, cyclohexane was the unique product with a phenol conversion of 100%. Under 1.0 MPa H₂ pressure, the selectivities to the reaction products were 49.4% for cyclohexane, 44.0% for cyclohexanone and 6.5% for benzene. By further decreasing the H₂ pressure to 0.2 MPa, the selectivity to benzene increased to 15.6% accompanied with 2.6% selectivity to cyclohexane and 81.8% selectivity to cyclohexanone. These results revealed that both path A and path B are the coexistent reaction pathways when reacting in *n*-octane, but path A is predominant.

The recyclability of the Pd/NaY catalyst was estimated by successively reacting for five runs. After each run, the catalyst was centrifuged and used directly for the next run. As shown in Fig. 6a, the conversion of phenol and the selectivity to cyclohexane could be preserved at about 95% and 71% after five-run tests with *n*-octane as the solvent. When artificially controlling the phenol conversion to be less than 100% in *n*-octane during catalytic stability study, the dominant product cyclohexane would be accompanied with the intermediate products of benzene, cyclohexanol and cyclohexanone, which further undergo hydrogenation or hydrodeoxygenation to form cyclohexane. In EtOH (Fig. 6b), however, the conversion of phenol was about 78% with 92% selectivity to cyclohexanol. No decrease in the catalytic activity was observed. The Pd content in the spent catalyst (1.96 wt%) is nearly identical with that in the fresh one by ICP measurement, indicating that no metal leaching occurred during the reaction. Moreover, XPS, TEM and PXRD characterization showed that the spent Pd/NaY catalyst was almost the same as the fresh one (Fig. S4–S6†), suggesting that Pd/NaY is a robust catalyst for the hydrogenation of phenol.

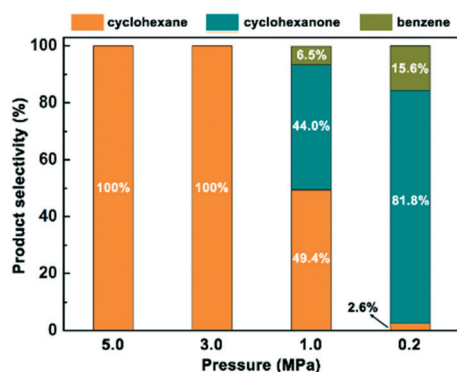


Fig. 5 The product distribution for phenol conversion under different H₂ pressures. Reaction conditions: 0.1 g catalyst, 1.0 g phenol, 70 mL *n*-octane, 235 °C, 4.0 h.

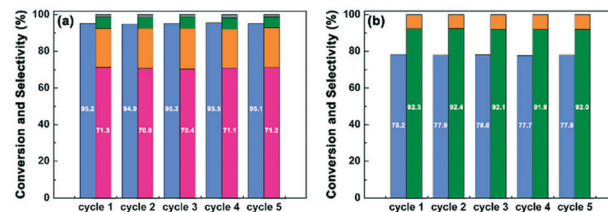


Fig. 6 The recyclability of the Pd/NaY catalyst for phenol conversion in (a) *n*-octane and (b) EtOH. Reaction conditions: 0.1 g catalyst, 1.0 g phenol, 70 mL solvent, 5.0 MPa H₂, 235 °C, 20 min in *n*-octane and 4.0 h in EtOH. Phenol conversion (blue) and selectivity to cyclohexane (pink), cyclohexanone (orange), cyclohexanol (green) and benzene (gray).

Adsorption of phenol over the Pd/NaY catalyst in the two solvents was conducted to investigate the solvent effect on the interaction with the catalyst surface. Considering the difficulty in the measurement at high temperature, the adsorption experiments were carried out at room temperature (Fig. 7). With the increase of phenol concentration in both solvents, the adsorption capacity of phenol increased gradually. At a phenol concentration of 0.25 g L⁻¹, the adsorption capacity in EtOH was equivalent to that in *n*-octane due to the sufficient adsorption sites on Pd/NaY available. By further increasing the phenol concentration, the adsorption capacity of phenol in *n*-octane was much higher than that in EtOH, suggesting that the polar solvent molecules are likely to competitively occupy the adsorption sites (acid sites) with phenol. As a consequence, the dehydration of phenol was greatly suppressed.

For the conversion of phenolic compounds, the dehydration reaction is critical, which determines the selectivity towards alcohol or alkane species.^{38,39} The dehydration mechanism of cyclohexanol was investigated by DFT calculations. The possible reaction pathways for the dehydration of cyclohexanol both in *n*-octane and in EtOH were considered (Fig. 8), but the results show that solvents have an almost negligible effect on the reaction energy barrier. Our calculations revealed that in the absence of zeolite, the direct dehydration of cyclohexanol seems infeasible with high free

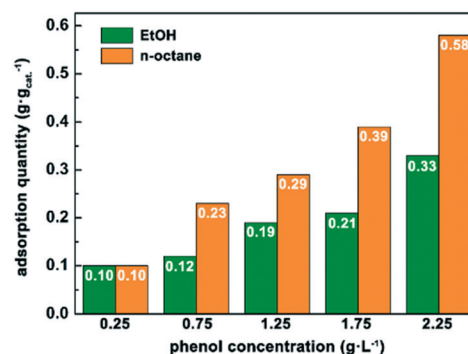


Fig. 7 The adsorption quantity of phenol over the Pd/NaY catalyst in the solvents EtOH and *n*-octane with different phenol concentrations. Reaction conditions: 0.2 g catalyst, 40 mL solvent, 25 °C, 20 h.

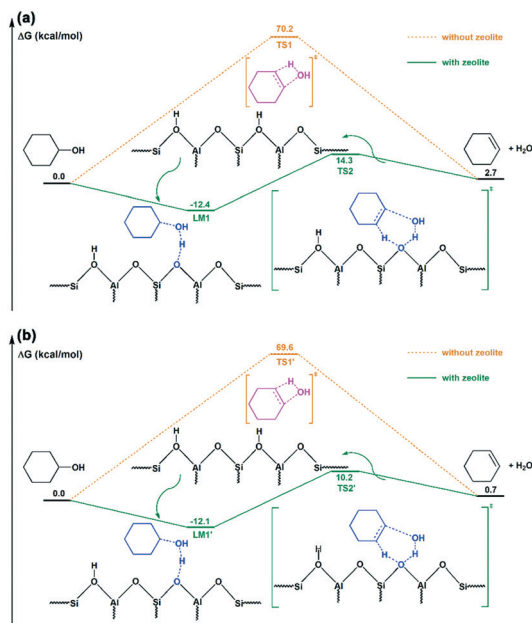


Fig. 8 DFT calculations of the reaction pathways for the dehydration of cyclohexanol without or with the catalysis of the NaY zeolite in the solvents (a) *n*-octane and (b) EtOH (values are relative Gibbs free energies ΔG in kcal mol⁻¹).

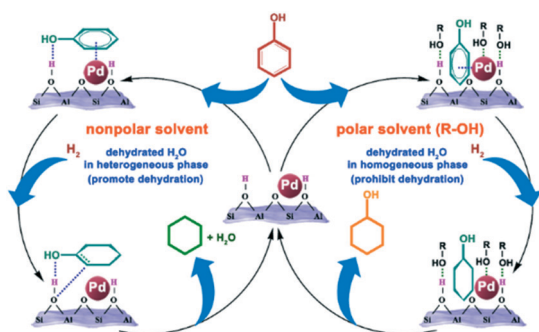


Fig. 9 The proposed catalytic mechanism of the solvent-driven selectivity for the phenol conversion over the bifunctional Pd/NaY catalyst.

energy barriers of 70.2 kcal mol⁻¹ (TS1) in *n*-octane and 69.6 kcal mol⁻¹ (TS1') in EtOH. Brønsted acids are essential to catalyze the dehydration of cyclohexanol,⁴⁰ and acidic zeolites are effective catalysts for dehydration reactions. As shown in Fig. 8, with the aid of the zeolite, the dehydration of cyclohexanol becomes kinetically favorable under the catalysis of the Brønsted acid sites of the zeolite, in which the free energy barriers are reduced to 26.7 kcal mol⁻¹ (TS2) in *n*-octane and 22.3 kcal mol⁻¹ (TS2') in EtOH. The DFT calculation results, however, could not rationalize the observed different selectivities in different solvents as the reaction mechanisms in *n*-octane and EtOH are similar.

It is worth noting that the dehydration of cyclohexanol to cyclohexene is thermodynamically unfavourable, leading to a very limited yield for hydrocarbons when the reactants and products are in a homogeneous phase. As shown in Fig. 9,

the interaction between polar solvent molecules and the Pd surface decreases the reactivity of the reactants because of the competitive adsorption with phenol. Besides, the competitive adsorption by the polar solvent molecules makes the hydroxy group of phenol inaccessible to the acid sites, leading to “nonplanar” adsorption on the Pd/NaY catalyst, which effectively intercepts the process of cyclohexanol dehydration. More importantly, cyclohexanol, the dehydrated products of cyclohexene and water are dissolved easily in the polar EtOH solvent, leading to the very little formation of hydrocarbon products. Meanwhile, in nonpolar *n*-octane without competitive adsorption, the hydroxy group of phenol could access the acid sites with “planar” adsorption on the Pd/NaY catalyst, resulting in the occurrence of cyclohexanol dehydration. Moreover, cyclohexanol and cyclohexene are soluble but water is insoluble in nonpolar *n*-octane. The produced water is thus timely expelled and turned into the vapor phase, promoting the dehydration reaction of cyclohexanol.

3. Conclusions

In summary, we have demonstrated that the Pd/NaY catalyst, featuring encapsulated Pd NPs in the pores of the NaY zeolite with abundant acid sites, could be used as a bifunctional catalyst for efficient hydrogenation of phenol. Under the identical conditions, 100% selectivity to cyclohexane could be achieved when reacting in nonpolar *n*-octane, while 92.3% selectivity to cyclohexanol was achieved in polar EtOH. The polarity of the solvent has a decisive influence on the hydrogenation reaction mechanism, which not only affects the competitive adsorption capacity but also the adsorption manner of phenol on the acid sites and the Pd nanoparticles on the Pd/NaY catalyst. DFT calculations further show that different solvents have an almost negligible effect on the reaction energy barriers but highly affect the hydration reaction of cyclohexanol if the trace amount of water formed could not be timely removed from the catalytic system. This solvent-driven effect provides a facile strategy for the selective conversion of other phenolics into desired alcohol or alkane products.

Conflicts of interest

There are no conflicts to declare.

Acknowledgements

The project was supported by the National Key R&D Program of China (2019YFD1100602) and the National Natural Science Foundation of China (21978158 and 21973094).

Notes and references

- 1 Y. Wang, J. Yao, H. Li, D. Su and M. Antonietti, *Chem. Soc. Rev.*, 2011, **133**, 2362–2365.
- 2 L. Zhou, J. Xu, H. Miao, F. Wang and X. Li, *Appl. Catal., A*, 2005, **292**, 223–228.

- 3 S. Hu, M. Xue, H. Chen and J. Shen, *Chem. Eng. J.*, 2010, **162**, 371–379.
- 4 A. K. Suresh, M. M. Sharma and T. Sridhar, *Ind. Eng. Chem. Res.*, 2000, **39**, 3958–3997.
- 5 S.-C. Hu and Y.-W. Chen, *Ind. Eng. Chem. Res.*, 1997, **36**, 5153–5159.
- 6 T. Takahashi, T. Kai, H. Kimura and A. Inoue, *Mater. Trans.*, 2001, **42**, 1599–1602.
- 7 C. M. Cirtiu, A. F. Dunlop-Brière and A. Moores, *Green Chem.*, 2011, **13**, 288–291.
- 8 S. E. Lyubimov, M. V. Sokolovskaya, A. A. Korlyukov, O. P. Parenago and V. A. Davankov, *J. Iran. Chem. Soc.*, 2020, **17**, 1283–1287.
- 9 A. K. Talukdar and K. G. Bhattacharyya, *Appl. Catal., A*, 1993, **96**, 229–239.
- 10 C. Chen, P. Liu, M. Zhou, B. K. Sharma and J. Jiang, *Energies*, 2020, **13**, 846–858.
- 11 M. Tymchyshyn and C.-B. Xu, *Bioresour. Technol.*, 2010, **101**, 2483–2490.
- 12 K. V. R. Chary, D. Naresh, V. Vishwanathan, M. Sadakane and W. Ueda, *Catal. Commun.*, 2007, **8**, 471–477.
- 13 P. Claus, H. Berndt, C. Mohr, J. Radnik, E.-J. Shin and M. A. Keane, *J. Catal.*, 2000, **192**, 88–97.
- 14 I. Witońska, A. Królak and S. Karski, *J. Mol. Catal. A: Chem.*, 2010, **331**, 21–28.
- 15 D. Zhang, Y. Guan, E. J. M. Hensen, L. Chen and Y. Wang, *Catal. Commun.*, 2013, **41**, 47–51.
- 16 Y.-Z. Xiang, L.-N. Kong, C.-S. Lu, L. Ma and X.-N. Li, *React. Kinet., Mech. Catal.*, 2010, **100**, 227–235.
- 17 Y. Xu, Z. Peng, Y. Yu, D. Wang, J. Liu, Q. Zhang and C. Wang, *New J. Chem.*, 2020, **44**, 5088–5096.
- 18 C. Zhao, D. M. Camaioni and J. A. Lercher, *J. Catal.*, 2012, **288**, 92–103.
- 19 S. Velu, M. P. Kapoor, S. Inagaki and K. Suzuki, *Appl. Catal., A*, 2003, **245**, 317–331.
- 20 J. Zhong, J. Chen and L. Chen, *Catal. Sci. Technol.*, 2014, **4**, 3555–3569.
- 21 P. Yan, M. M.-J. Li, E. Kennedy, A. Adesina, G. Zhao, A. Setiawan and M. Stockenhuber, *Catal. Sci. Technol.*, 2020, **10**, 810–825.
- 22 G. Li, J. Han, H. Wang, X. Zhu and Q. Ge, *ACS Catal.*, 2015, **5**, 2009–2016.
- 23 M. V. Bykova, D. Y. Ermakov, S. A. Khromova, A. A. Smirnov, M. Y. Lebedev and V. A. Yakovlev, *Catal. Today*, 2014, **220–222**, 21–31.
- 24 H. Yun, Y. Lee, S. Son, M. Chung, M. Jang, E. J. Shin, S. Jung, W. Kwak, W. J. Jeong and H. G. Ahn, *J. Nanosci. Nanotechnol.*, 2017, **17**, 2776–2779.
- 25 Z. Luo, Z. Zheng, Y. Wang, G. Sun, H. Jiang and C. Zhao, *Green Chem.*, 2016, **18**, 5845–5858.
- 26 L. Wang, P. Ye, F. Yuan, S. Li and Z. Ye, *Int. J. Hydrogen Energy*, 2015, **40**, 14790–14797.
- 27 P. M. de Souza, R. C. Rabelo-Neto, L. E. P. Borges, G. Jacobs, B. H. Davis, T. Sooknoi, D. E. Resasco and F. B. Noronha, *ACS Catal.*, 2015, **5**, 1318–1329.
- 28 F. Li, B. Cao, W. Zhu, H. Song, K. Wang and C. Li, *Catalysts*, 2017, **7**, 145–155.
- 29 I. Urukova, J. Vorholz and G. Maurer, *J. Phys. Chem. B*, 2005, **109**, 12154–12159.
- 30 J. He, C. Zhao and J. A. Lercher, *J. Catal.*, 2014, **309**, 362–375.
- 31 X. Chen, K. Shen, D. Ding, J. Chen, T. Fan, R. Wu and Y. Li, *ACS Catal.*, 2018, **8**, 10641–10648.
- 32 W. Fu, L. Zhang, T. Tang, Q. Ke, S. Wang, J. Hu, G. Fang, J. Li and F. S. Xiao, *J. Am. Chem. Soc.*, 2011, **133**, 15346–15349.
- 33 M. Aimen Isa, M. Hanif Halim, T. L. Chew and Y. F. Yeong, *IOP Conf. Ser.: Mater. Sci. Eng.*, 2020, **736**, 052019.
- 34 R. Wojcieszak, M. J. Genet, P. Eloy, P. Ruiz and E. M. Gaigneaux, *J. Phys. Chem. C*, 2010, **114**, 16677–16684.
- 35 A. Maghfirah, M. M. Ilmi, A. T. N. Fajar and G. T. M. Kadja, *Mater. Today Chem.*, 2020, **17**, 2468–5194.
- 36 P. C. D. Mendes, R. Costa-Amaral, J. F. Gomes and J. L. F. Da Silva, *Phys. Chem. Chem. Phys.*, 2019, **21**, 8434–8444.
- 37 X. Li, L. Cheng and X. Wang, *Res. Chem. Intermed.*, 2018, **45**, 1249–1262.
- 38 L. Nie, P. M. de Souza, F. B. Noronha, W. An, T. Sooknoi and D. E. Resasco, *J. Mol. Catal. A: Chem.*, 2014, **388–389**, 47–55.
- 39 X. Zhu, L. Nie, L. L. Lobban, R. G. Mallinson and D. E. Resasco, *Energy Fuels*, 2014, **28**, 4104–4111.
- 40 A. Clearfield and D. S. Thakur, *J. Catal.*, 1980, **65**, 185–194.